



*Semester End Project:
Redesign of Filter/Amplifiers to Incorporate
Filters with Different Cutoff Frequencies*

Group M5
Mariza Clement
Richard Kiok
Jinwah Lau
Mark Phong

Submitted December 12, 1997

SPECIFIC AIMS

1. To build a 2-pole Butterworth filter for filtering human EKG signals.
2. To find the properties of the filter using simple signals (sine and square).
3. To find the optimal cutoff frequency for EKG filtration.

ABSTRACT

In this project, analog 2-pole Butterworth filters were built to filter human EKG signals. Four filters designed with cut off frequencies near 1, 10, 40 and 70 Hz were built using variable resistors and fixed capacitors in order to facilitate the changing of the cut-off frequencies. The actual cut-off frequency and passband of each filter was initially determined using sine and square wave signals. An EKG was inputted into each filter and the optimal cutoff frequency was determined to be 10 Hz. The phase shift was determined to be linear, with a multiple R-value of 0.9998. The attenuation rate per decade of the filter was determined to be less than the ideal -40dB per decade, for a 2-pole filter.

BACKGROUND

A Butterworth filter is a signal processor that amplifies signals in a band of frequencies and attenuates signals in another band. The low-pass filter passes and can amplify signals below its cut off frequency, attenuates and rejects high frequency components of the stopband after the cut off frequency (ω_c). Low pass Butterworth filters are derived from a gain response shown in equation 1,

$$T_n(j\omega) = \frac{|K_o|}{\sqrt{1 + \left(\frac{\omega}{\omega_c}\right)^{2n}}} \quad \text{Eq. 1}$$

where $T_n(j\omega)$ is the transfer function, ω is the input frequency, n is the number of poles in $T_n(s)$, and K_o is the passband gain. For a two pole Butterworth filter, a second order polynomial of the form $(s/\omega_c)^2 + 2\zeta(s/\omega_c) + 1$ produces a gain function

$$|T_2(j\omega)| = \frac{|K_o|}{\sqrt{\left(1 - \frac{\omega^2}{\omega_c^2}\right)^2 + 2\zeta\left(\frac{\omega}{\omega_c}\right)^2}} \quad \text{Eq. 2a}$$

which is equivalent to

$$T_2(j\omega) = \frac{|K_o|}{\sqrt{1 + (4\zeta^2 - 2)\left(\frac{\omega}{\omega_c}\right)^2 + \left(\frac{\omega}{\omega_c}\right)^4}} \quad \text{Eq. 2b}$$

This form of the transfer function is equivalent to equation 1 provided that $n=2$ and $2\zeta=\sqrt{2}$. The normalized denominator polynomial for a second order filter is $(s^2 + 1.414s + 1)$. This polynomial sets the design parameters of ω_c equal to s and ζ equal to $1.414/2$, which equals 0.707 . The prototype for a two pole Butterworth filter is presented in figure 1.

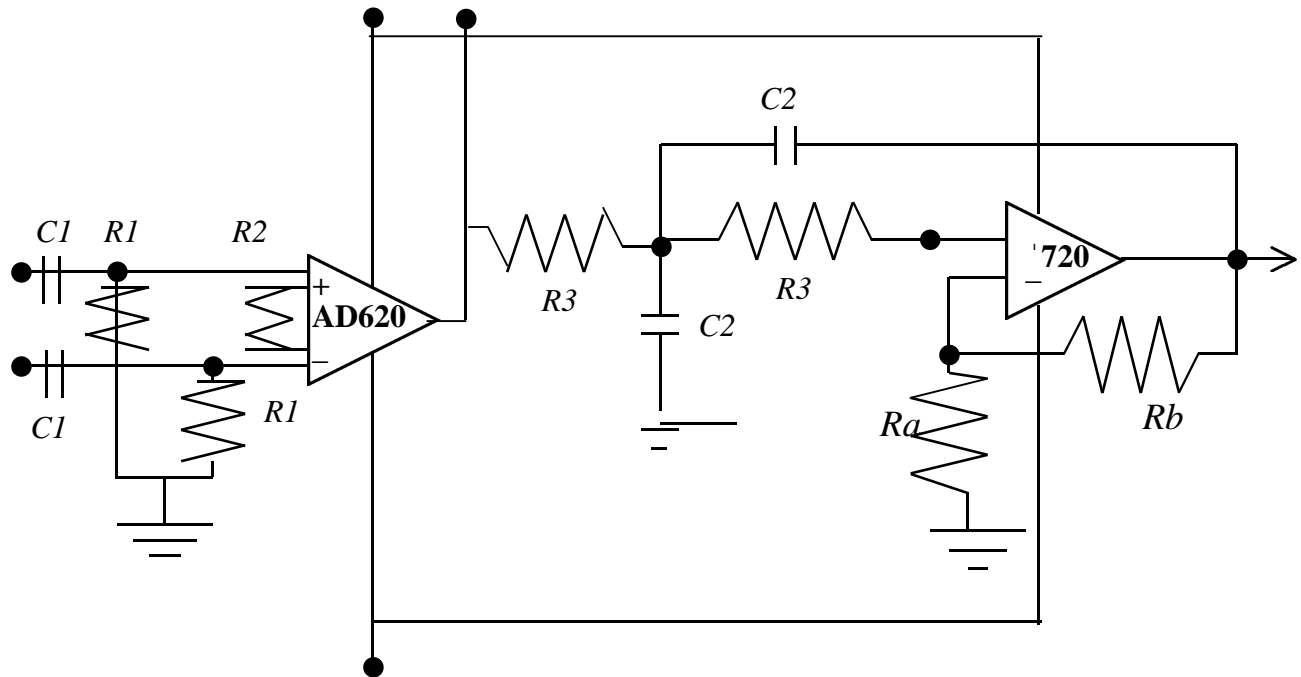


Figure 1: Stage Prototype of 2 Pole Butterworth Filter with Amplifier.

Given this design, the cut off frequency is defined by equation 3 and the damping ratio (K) is defined by equation 4.

$$\omega_c = 1/RC \tag{Eq. 3}$$

$$K = 3 - 2\xi = 1.586 \tag{Eq. 4}$$

R_a and R_b control the gain, which is dependent on the stage damping ratio of a two pole filter shown in equation 5.

$$R_a = (K - 1)R_b \tag{Eq. 5}$$

In a two pole Butterworth filter, only one stage is required for its construction. This indicates that the passband gain will be equal to the stage damping ratio.

MATERIALS AND EQUIPMENT

1. Protoboard
2. Resistors (1M Ω , 100 Ω , variable resistors)
3. Capacitors (10 μ F, 100 μ F)
4. Labview EKGRecorder.VI
5. Virtual bench oscilloscope and function generator
6. Red Dot Electrodes
7. Patient Isolator

R1	1 M Ω
R2	100 Ω
R3	Variable
Ra	58.6 Ω
Rb	100 Ω
C1	10 μ F
C2	100 μ F

Figure 1b: Resistor and capacitor values corresponding to Figure 1.

METHODS

Choosing a filter design

In choosing a design of a low pass 2 pole Butterworth filter, several items were taken in consideration. First, the values of the resistors and capacitors needed to be found or calculated, and second, the effect of gain on the signal needed to be identified. The first filter built was modeled from Webster from which the values of the resistors were calculated using a set capacitor value and indicated multiples, $0.707 \cdot R_1$ and $1.414 \cdot R_2$. This model did not indicate the effects of gain nor did it indicate a method of calculating the gain. The different values of the resistors also posed as a question as to the effects they would have on filtering a signal. Other literature indicated that the values of the resistors and the values of the capacitors should be the same within each pole of the filter.

The second and final model that was built included two additional resistors that allowed for feedback related to the gain. Values of resistance and capacitance were calculated, and the filter was built according to specifications found in Thomas and Rosa. Since the values for R_3 (figure 1) must be equal and changed between each filter, variable resistors were used instead of building four separate filters. In addition an amplifier based from the BE 309 lab manual was added to amplify the EKG signal. The following table notes the resistor values used in the low pass 2 pole Butterworth design with a capacitance of $100\mu\text{F}$, calculated from equation 3.

Target Cut Off Frequency (Hz)	Resistor Values R_3 (ohms)
1	1591.5
10	159.2
40	39.8
70	22.7

Table 1: Filter Design Specifications

Aquiring Data

The Virtual bench oscilloscope and function generator were used to test the 2 pole Butterworth filter. The function generator allowed for the input of varying frequencies of sine and square waves. The unfiltered signal was fed into channel one of the oscilloscope and the filtered signal was inputted into channel two so that measurements could be taken of both the unfiltered and filtered signal. Initial testing of the filter included varying the input frequency and observing the effects of the filter in confirming the theoretical cutoff frequency. Knowing that the filter functioned properly, V peak-peak was recorded for input frequencies of 1-100 Hz in increments of 5 Hz for both sine and square waves. The ratio of filtered Vp-p and unfiltered Vp-p was then used to plot $\log (V_o/V_i)$ vs. input frequency.

Labview EKGRecorder.VI was used in recording real human EKG data. In this portion of the experiment, an amplifier was added onto the 2 pole Butterworth filter to ensure a distinguishable EKG signal. Unfiltered and filtered signals were also recorded, with the unfiltered signal inputted into Labview from the patient isolator and the filtered signal inputted in after passing through the amplifier and filter. 200 samples were taken at 30 samples/second. Measurements from Labview were saved and the graphical comparisons were made of the unfiltered and filtered signals. PQRST was indentified, filtered Vp-p/unfiltered Vp-p, and phase shifts were analyzed.

RESULTS

Varying the input frequency of sine and square waves, while measuring the peak to peak voltage enabled the calculation of the cutoff frequencies. The cutoff frequency was calculated by the linear form of the transfer function of a two pole Butterworth filter, as shown in equation 6, where K_o is equal to 1.

$$\log(V_{out}/V_{in}) = -n\log(\omega) + n\log(\omega_c) \quad (6)$$

This equation takes the basic empirical form $y=mx+b$ where $y = \log(V_{out}/V_{in})$, $m=-n$, $x= \log(\omega)$ and $b= n\log(\omega_c)$ since both n and ω_c are constants. A semilogarithmic plot exentuates the relationship between the transfer function and frequency. The results of inputting a sine and square wave into the filter built with a 1 Hz cut off is shown in figure 2.

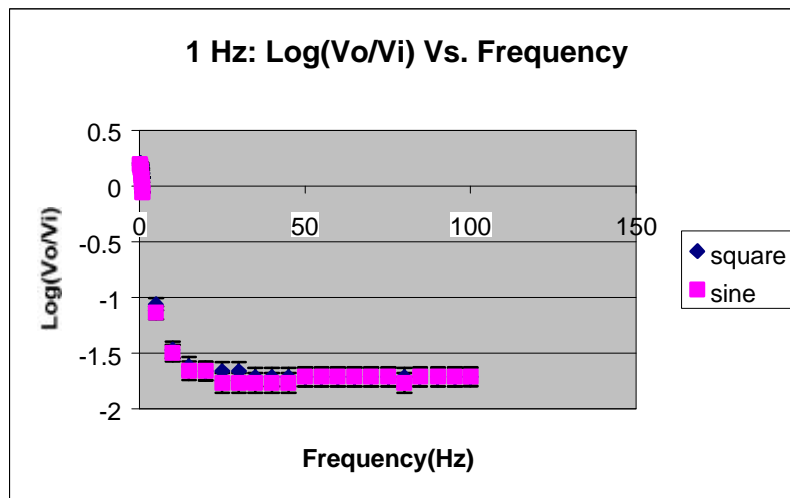


Figure 2. Target 1 Hz Cut Off: Log (Vout/Vin) as a Function of Frequency

Figure 2 shows a decreasing relationship between the transfer function and input frequency, which begins to level off at approximately 15 Hz. Only the region that exhibited attenuation was used to find the cut off frequency. Using equation 6, a linear regression of the region of attenuation (from 0.5 to 15 Hz) of $\log(V_{out}/V_{in})$ vs. $\log(\omega)$ was conducted.

The linear regression of these data points was performed, and figure 4 presents the regression of the square wave with a 1 Hz targeted cutoff.

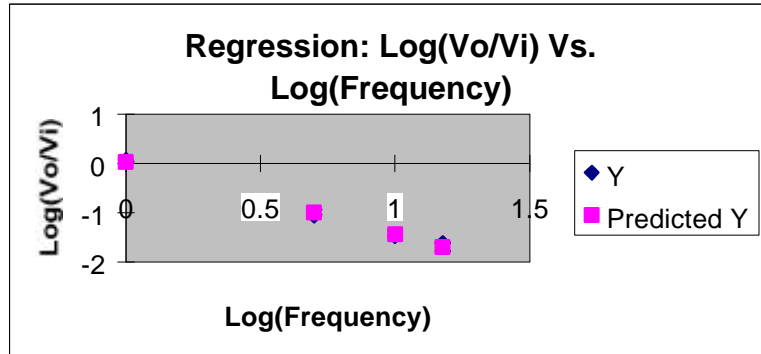


Figure 3: Target 1 Hz Cutoff: Linear Regression Between 1 to 15 Hz for Square Wave Data

The linear regression of figure 3 had a multiple R-value of 0.996, with a standard error of 0.0818. The slope of the region is -1.472 with an upper and lower 95% confidence level of -1.079 and -1.864, respectively. The intercept of this graph is 0.0401 with an upper and lower 95% confidence level of 0.372 and -0.292, respectively. Error bars on figure 4 are too small to be seen. Algebraic manipulation of equation 6 gives equation 7 for angular frequency.

$$\omega_c = 10^{(\text{intercept}/-1*\text{slope})} \quad \text{Eq. 6}$$

Solving for ω_c gives 1.0647. The same technique was used to analyze the sine wave data and data from the filters with estimated cut off frequencies of 10, 40 and 70 Hz. Results of the regression statistics for the square and sine data are in tables 2 and 3. The semilogarithmic plot of amplitude ratio as a function of frequency for the filter with a target cut off frequency of 10 Hz is displayed in figure 5.

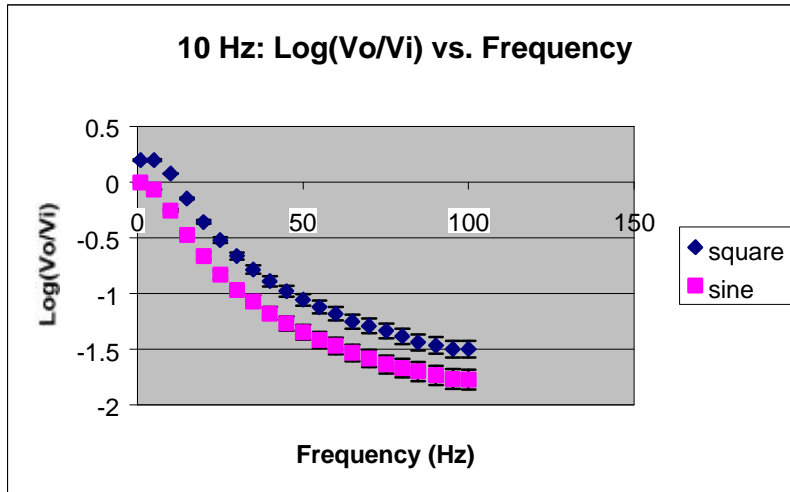


Figure 4: Target 10Hz Cut Off: Log of Amplitude Ratio as a Function of Frequency

The first two points of figure 4 represent the passband. After which, the output/input ratio attenuates until about 90 Hz. A linear regression of the $\log(V_{out}/V_{in})$ vs the log of frequency between 10-90 Hz was conducted. The results of the regression are in tables 2 and 3. Figure 6 shows the nature of the passband gain.

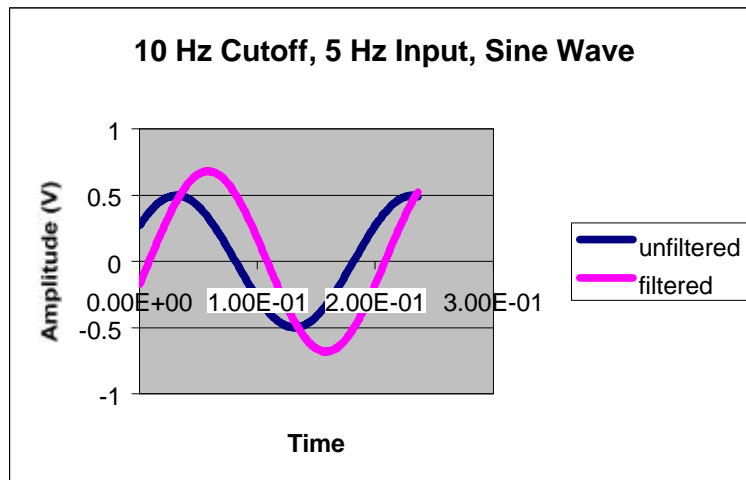


Figure 6: Passband Gain

Figure 6, illustrates the active nature of the circuit. Averaging the peak to peak ratio for frequencies under the cut off frequency and finding their standard deviation resulted in

the passband gain. The input signal is amplified by a factor of 1.57 ± 0.01 for frequencies under the cut off frequency. Passband gain for all of the filters is summarized in tables 4 and 5. Figure 7, presents the results of inputting a square and sine wave into the filter with a target cut off frequency of 40 Hz.

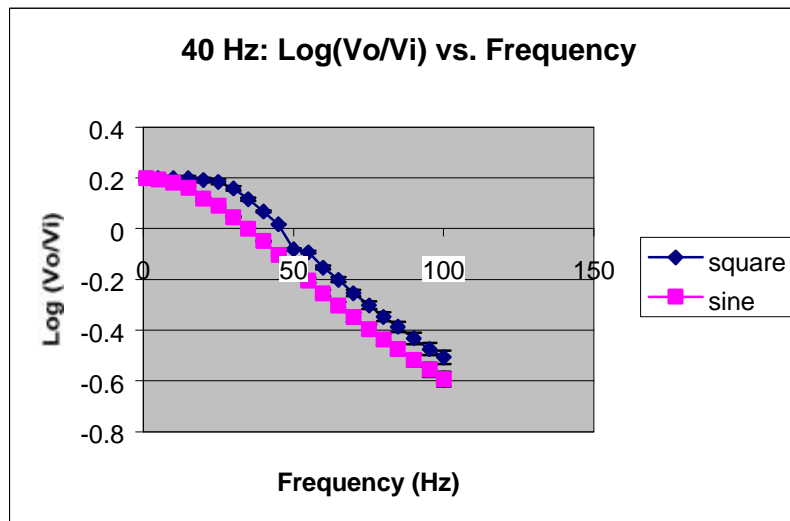


Figure 7: Target 40Hz Cutoff : Log of Amplitude Ratio as a Function of Frequency

In figure 7, a passband region is shown until 25 Hz for the square data. From 25 to 95 Hz, the filter attenuates the signal. The passband region of the sine data appears shorter than the square wave, but follows the same slope. Again, a linear regression of the log-log curve was taken of the area of attenuation. The results of the regression and cut off frequency are given in table 1. Inputting a square wave into the targeted 70 Hz filter resulted in Figure 8.

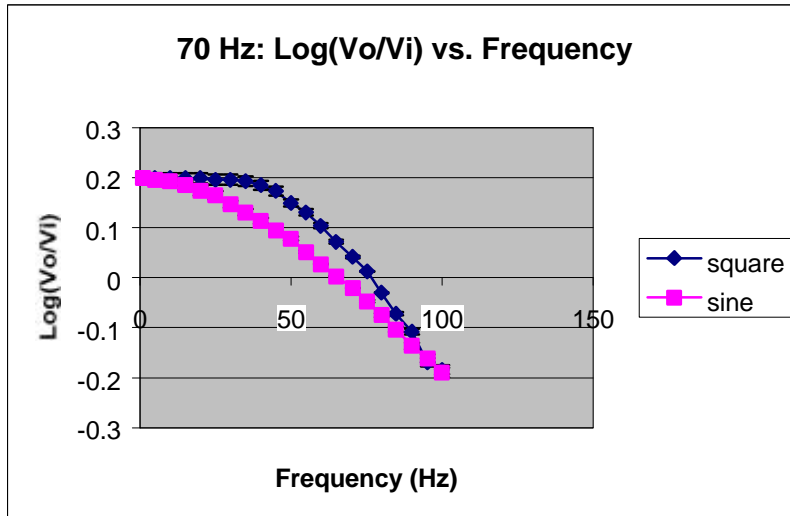


Figure 8: Target Cutoff 70 Hz: Log of Amplitude Ratio as a Function of Frequency

The passband region of the square data in figure 8 lasts until a frequency of 45 Hz is inputted. Then the amplitude ratio attenuates until 90 Hz. Analysis of the sine data shows a clear passband region between 1-25 Hz and begins to slope to an attenuation region until 90 Hz. Again, the results of the log-log regression are in Table 1 and 2.

Filter :Theoretical Cutoff Frequency (Hz)	1	10	40	70
Multiple R	0.996	0.999	0.992	0.989
Standard Error	0.0818	0.020	0.027	.016
Slope	-1.47 ± 0.09	-1.65± 0.02	-1.31± 0.05	-1.35 ± 0.08
Upper 95%	1.08	1.62	1.20	1.17
Lower 95%	1.86	1.69	1.41	1.53
Intercept	0.04 ±0.07	1.77± 0.03	2.14± 0.09	2.53 ± 0.15
Upper 95%	0.37	1.83	2.33	2.88
Lower 95%	-0.29	1.71	1.96	2.18

Table 2: Summary of Regression Statistics for Square Wave

Filter :Theoretical Cutoff Frequency (Hz)	1	10	40	70
Multiple R	0.995	0.999	0.998	0.999
Standard Error	0.092	0.020	0.011	0.996
Slope	-1.29±0.07	-1.63±0.02	-1.34±0.03	-1.00±0.04
Upper 95%	0.17	1.58	1.27	0.901
Lower 95%	0.023	1.67	1.41	1.11
Intercept	0.17±0.06	1.42± 0.03	2.11±0.05	1.83±0.07
Upper 95%	-0.124	1.49	2.24	2.03
Lower 95%	-0.414	1.35	2.00	1.63

Table 3: Summary of Regression Statistics for Sine Wave

The regression statistics signify that the regions of attenuation are statistically linear, with multiple R-values near 1. Recalling that the relationship between the slope, intercept and cut off frequency from equation 6; that is the slope equals negative n and the intercept $b = n \log(\omega_c)$. Using table 1, ω_c was solved for each of the filters and are displayed in table 2. Error due to the precision of the instruments was calculated using the regression statistics. The differential technique was applied to equation 7 resulting in equation 8 for the precision error.

$$d(vc) = \frac{10^{\frac{b}{n}} \ln(10) db}{n} - \frac{10^{\frac{b}{n}} b \ln(10) dn}{n^2} \quad \text{Eq. 7}$$

where dn is the error in the slope, db is the error in the y intercept taken from the regression statistics in tables 2 and 3.

Target Cut Off Frequency (Hz)	Experimental Cut Off Frequency (Hz)	Error (%)	Precision Error (%)	PassBand Gain
1	1.06 ± 0.02	6.47	2.83	1.59 ± 0.00
10	11.73 ± 0.17	17.30	1.45	1.57 ± 0.00
40	43.79 ± 0.51	9.46	1.16	1.58 ± 0.00
70	74.15 ± 0.28	5.93	0.38	1.58 ± 0.0005

Table 4: Summary of Square Wave Results

Target Cut Off Frequency (Hz)	Experimental Cut Off Frequency (Hz)	Error (%)	Precision Error (%)	PassBand Gain
1	0.74 ± 0.09	26.00	11.49	1.57 ± 0.01
10	7.55 ± 0.16	24.50	2.12	1.57 ± 0.01
40	37.55 ± 0.42	6.13	1.13	1.55 ± 0.03
70	66.64 ± 0.48	4.88	0.72	1.57 ± 0.01

Table 5: Summary of Sine Wave Results

EKG Results

Using the filters described in the preceding section of the results, the EKG of a human subject was studied. The EKG was taken at a sampling rate of 30 Hz for 6.67 sec., giving a total sample count of 200 per trial. Filters with cutoff frequencies of 1, 10, 40, and 70 Hz were used in an attempt to remove unwanted noise. The following graphs have had the mean value subtracted from every point in order to remove the DC-offset, thus centering each graph at zero. One representative trial (filtered and unfiltered EKG) from each filter is provided for comparison.

1 Hz Cutoff Data

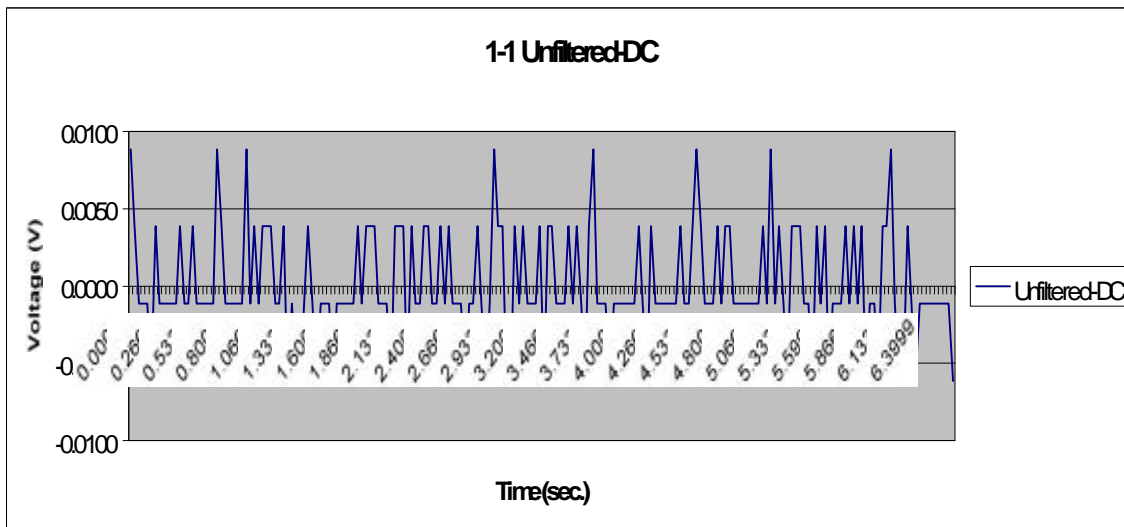


Figure 8: Graph of an unfiltered EKG.

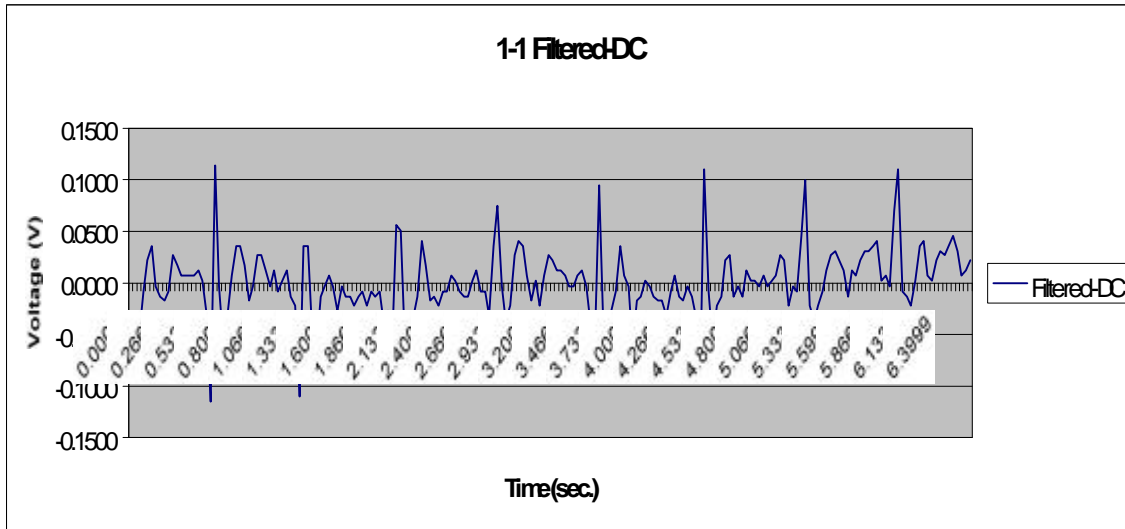


Figure 9: Graph of EKG shown in Figure 8 after passing through the 1 Hz cutoff filter.

In Figure 8, the QRS complex of the EKG can be distinguished with some difficulty. Yet, there is still significant corruption in the signal. Figure 9 demonstrates the same EKG shown in Figure 8 after passing the signal through the 1 Hz cutoff frequency filter. Figure 9 shows the QRS complex clearly while the P and T waves are still corrupted.

10 Hz Cutoff Data

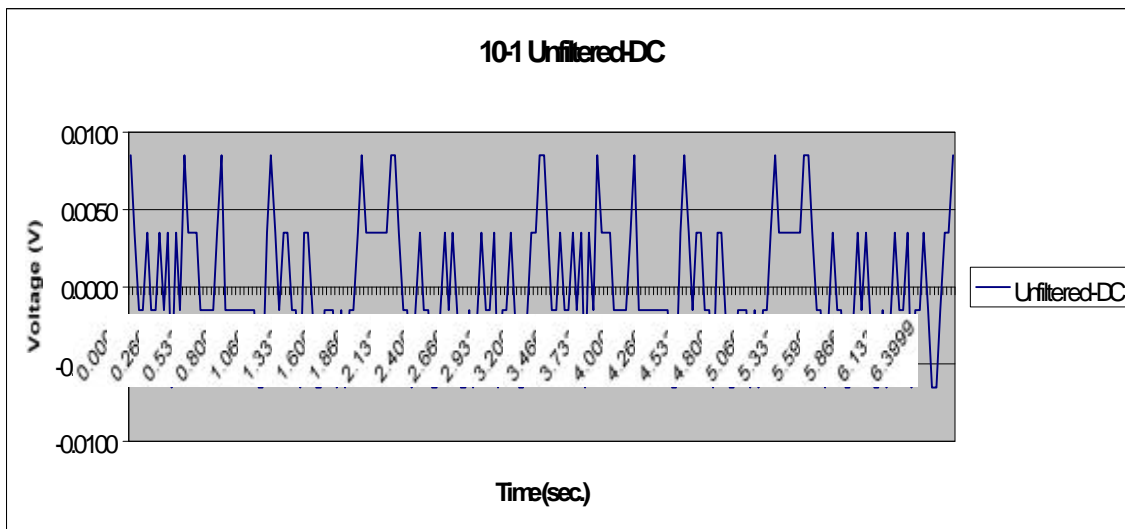


Figure 10: Graph of an unfiltered EKG.

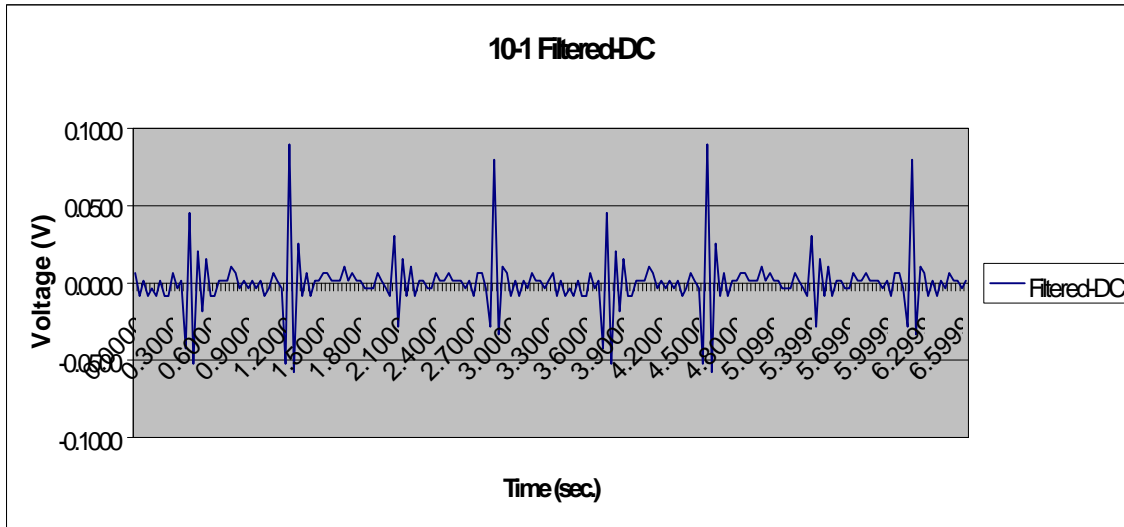


Figure 11: Graph of EKG shown in Figure 10 after passing through the 10 Hz cutoff filter.

Figure 10 shows the unfiltered EKG. It looks very similar to the unfiltered EKG shown in Figure 8. Figure 11 shows the same signal after passing it through the 10 Hz cutoff frequency filter. In Figure 11, the QRS complex and the T wave can be easily distinguished. The P wave is clear in some, but not all, of the signals.

40 Hz Cutoff Data

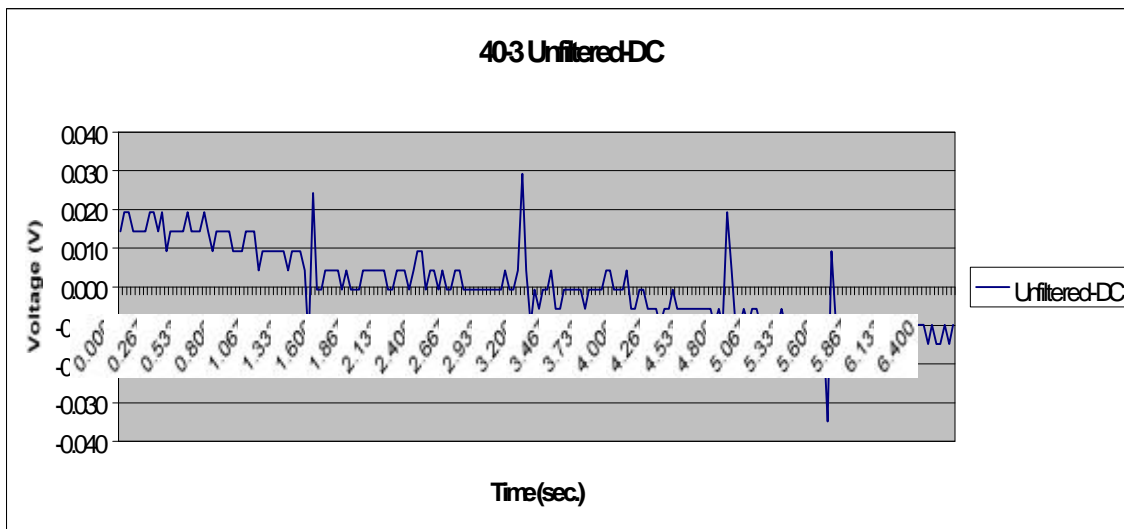


Figure 12: Graph of an unfiltered EKG.

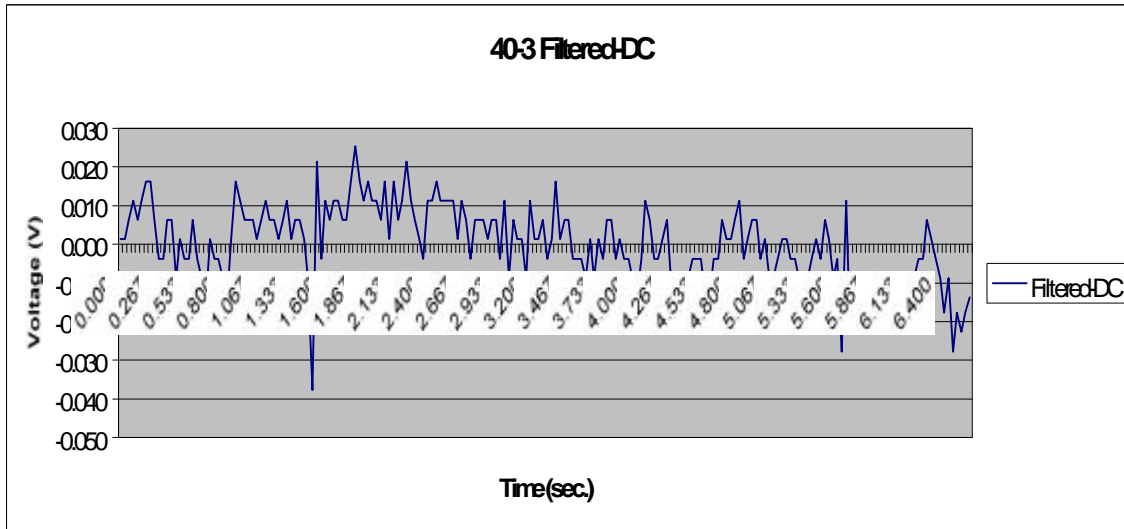


Figure 13: Graph of EKG shown in Figure 12 after passing through the 40 Hz cutoff filter.

Figure 12 shows the unfiltered EKG. Unlike Figures 8 and 10, some features of an EKG can be seen, notably regularly spaced R peaks. There is still a significant portion of the noise in the signal. Figure 13 shows the EKG shown in Figure 12 after passing the signal through the 40 Hz cutoff frequency filter. The filtered signal appears to be much more corrupted than the unfiltered signal, and no portion of the normal EKG can be distinguished.

70 Hz Cutoff Data

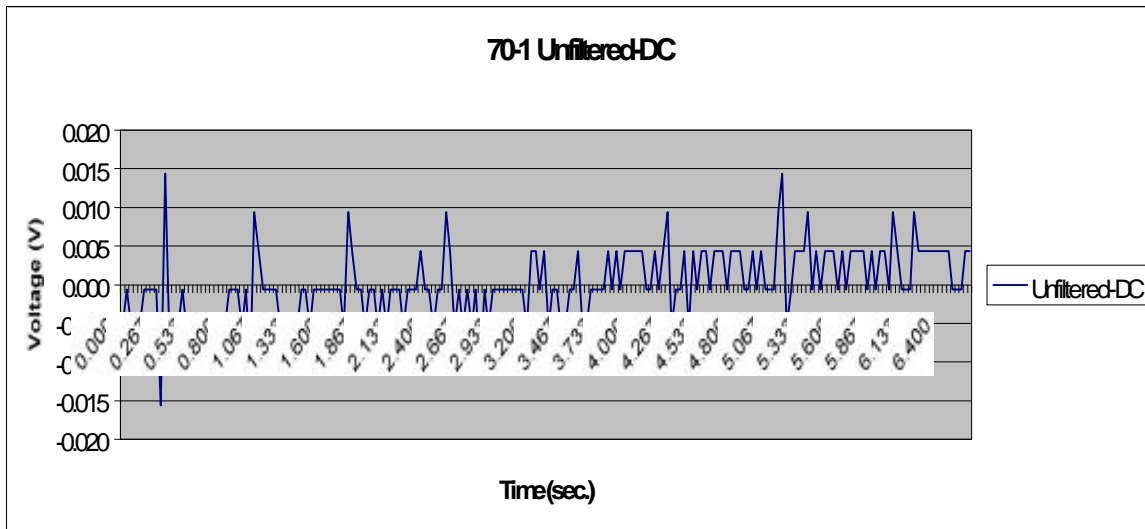


Figure 14: Graph of an unfiltered EKG.

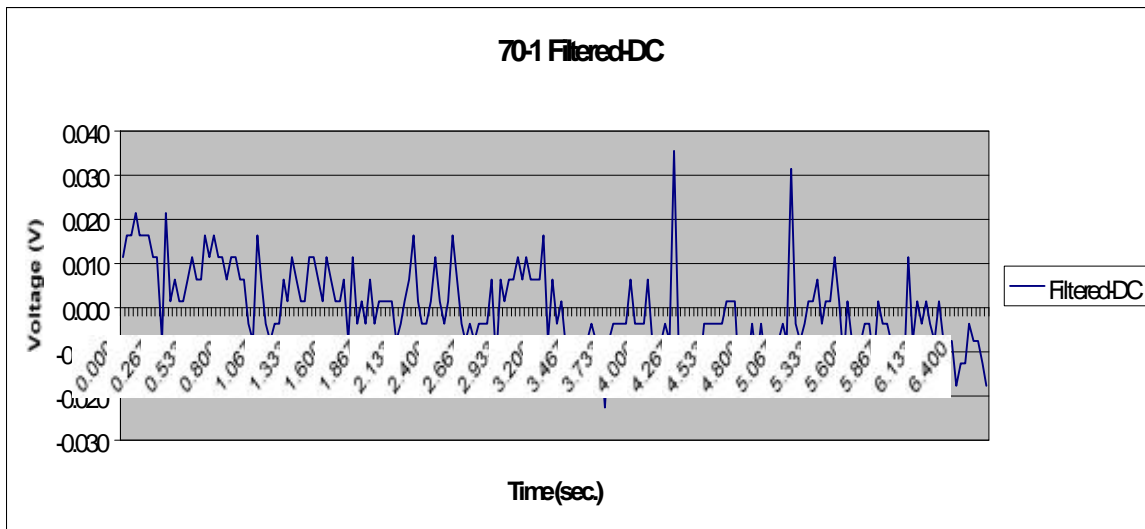


Figure 15: Graph of EKG shown in Figure 14 after passing through the 70 Hz cutoff filter.

Figure 14 shows the unfiltered EKG. Noise is evident between what seems to be a series of R peaks that would be expected in the normal EKG. Other aspects of the EKG are indeterminable. Figure 15 shows the EKG after filtration using the 70 Hz cutoff frequency filter. Noise is still evident, yet reduced, especially between the two large R peaks around 4.25 and 5.10 seconds. Other features of the EKG are disrupted or absent altogether.

Cutoff (Hz)	Vo/Vi	Filtered Vp-p (V)	Unfiltered Vp-p (V)	Phase Angle (Filtered)	Phase Angle (Unfiltered)	Phase Shift (rad.)
1	10.623	0.1715	0.0161	0.4164	-0.1769	-0.5933
10	5.6309	0.0915	0.0163	0.3542	-0.1379	-0.4921
40	1.6021	0.0475	0.0297	0.6926	0.4816	-0.2110
70	1.4929	0.0359	0.0241	0.3533	0.4407	0.0875

Table 6: Summary table of EKG results.

Table 6 presents a summary of the results from the EKG trials. V_o is the output voltage from the filter (i.e. the filtered EKG), and V_i is the input voltage (i.e. the unfiltered EKG). All four filters present V_o/V_i ratios greater than unity, as would be expected with an active filter.

Phase angles were calculated using the coefficients from the FFT. The output of the FFT is in the form $a + bi$, where a is the real coefficient and b is the imaginary coefficient.

$$PhaseAngle = \arctan\left(\frac{-b}{a}\right) \quad \text{Eq. 8}$$

$$PhaseShift = PhaseAngle_{Unfiltered} - PhaseAngle_{Filtered} \quad \text{Eq. 9}$$

As in Experiment 2: The Electrocardiogram: Digital Filtration Analysis from the BE Laboratory III Manual, the phase angles were calculated from the coefficients of the first signal peaks, in order to standardize the process.

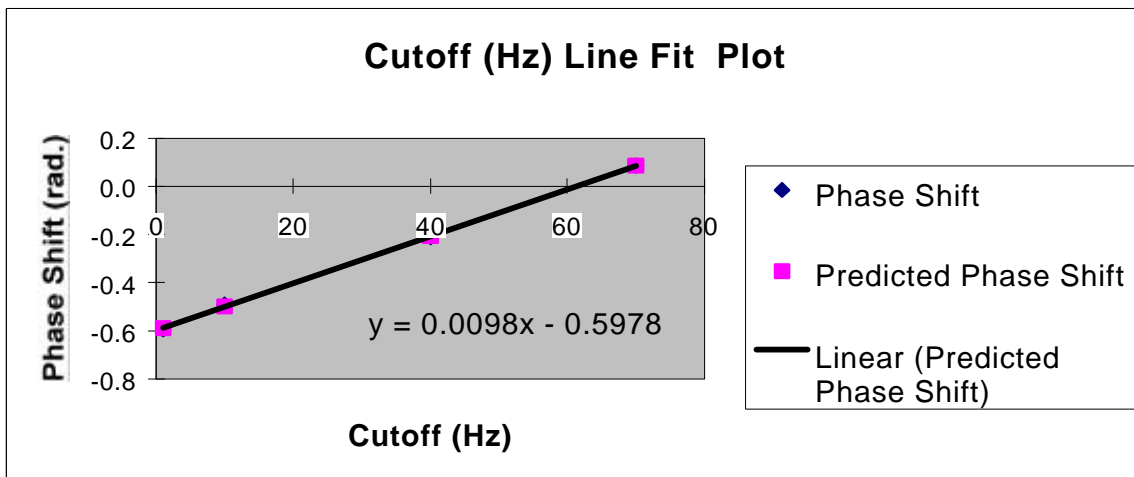


Figure 16: Plot of Phase Shift vs. Cutoff Frequency.

Figure 16 shows a linear relationship between cutoff frequency and phase shift as calculated from Equation XX. The multiple R-value of 0.9998 is very close to one, and the P-value of 8.62E-5 indicates that this relationship is not due to random chance.

<i>EKG</i>	<i>P-Q</i>		<i>QRS</i>			<i>T</i>
1	0.1556	95% CI	0.0667	95% CI	0.4222	95% CI
2	0.1555	0.0127	0.0667	0.0000	0.4000	0.0606
3	0.1556	upper 95% CI	0.0667	upper 95% CI	0.2556	upper 95% CI
4	0.1667	0.1771	0.0667	0.0667	0.3000	0.4072
5	0.1889	lower 95% CI	0.0667	lower 95% CI	0.3556	lower 95% CI
Average	0.1644	0.1518	0.0667	0.0667	0.3467	0.2861
Normal	0.12 - 0.2		0.0800		0.3500	

Table 7: Time intervals for the components of the EKG wave.

DISCUSSION

The experimental cutoff frequencies with inputted square waves were greater in all the filter settings of 1, 10, 40, and 70 Hz as compared to the theoretical cutoff frequencies. The differences in the experimental and theoretical cutoff frequencies ranged from 1.8-17.3%. In comparison, the experimental cutoff frequencies for an inputted sine wave were less than the theoretical cutoff frequency for all the filter settings ranging from 4.9-26%. The greater experimental cutoff frequency in the square wave is possibly due to the impossibility of generating a true step function since signal variables cannot transition from one value to another in zero time. Only an approximation of a step function can be made. With the sine wave, the attenuation begins earlier with a greater amount of error.

The larger error associated with using the sine wave is expected since the square wave is the sum of an infinite number of sine components whose frequencies are odd whole number multiples of the fundamental (f_0 , $3f_0$, $5f_0$,...). Noise exhibits slightly different frequencies, along with varying amplitudes and phase shifts. Since the square wave produces a function based on multiples of the fundamental frequency, any noise present will inherently be minimized. This is not the case with the sine wave as a sinusoidal function is more sensitive to variations in input frequency such as extraneous noise in the room. Physically comparing the graphs of log amplitude ratio vs. frequency, figures 7 and 8, the square wave shows a sharper transition at the cutoff frequency as compared to the sine wave, which may be also be attributed to the differences in the two wave forms.

The experimental values calculated for the number of poles do not match the theoretical 2 poles which was used as a constraint in building the filter. The only slope that begins to match the targeted 2 poles is the filter with targeted 10 Hz cutoff when it is rounded to the nearest whole number for both the sine and square waves. The poles of the other filter settings are less than 1.5, rounding to 1 pole. The discrepancy in poles signifies that the filter is a non-ideal 2-pole filter and exhibits an attenuation of less than -40dB/decade. The number of poles, ideally, should not affect the experimental cutoff frequency since attenuation occurs in the stopband after the cutoff frequency, but as

explained above, input square waves had a greater cutoff frequency and input sine waves had a smaller cutoff frequency compared to theoretical.

The passband gain calculated from the experimental data had an average value of 1.58 ± 0.0076 over 8 trials (square and sine wave inputs) which is significantly similar to the theoretical gain of 1.586 that was an inherent property of the filter.

Systematic errors in this experiment stem from the use of LabView in recording the peak to peak voltage readings. As a result, to minimize these errors LabView is programmed to take the average of several peak to peak voltage values while measuring amplitude. The function generator produces a rapidly flashing series of numbers and approximates the averages. Systematic uncertainty was minimized in data collection by these approximations and is assumed to be negligible. The error attributed to systematic uncertainty is quantifiable by the statistics presented in Table 4 and 5 from the linear regression of the log-log curves. As shown in the results section, the precision error in calculating the cutoff frequency decreases with increasing cutoff frequency. In the square wave input, the target 1 Hz cutoff frequency gives a precision error of 11.32%, and the target 70 Hz cutoff has a precision error of 0.38%. This trend is apparent in both the square and sine wave inputs. The calculation of the cut off frequency is dependent on logarithmic functions, thus any error present will be amplified while calculating f_c .

Random errors such as noise from the electrical connections and filter most likely contributed the largest source of error. Subtracting the systematic precision error from the total percent error gives the amount of random error, which ranges from 22.4% to 4.16%. The amount of random error is 55.8% to 93.6% greater than the systematic error.

Discussion of EKG Results

As seen in visual representation of the filtered and unfiltered signals in the results section of the report, the filter does not completely remove the noise component of the overall signal. In Figure 11, it can be seen that the 10 Hz cutoff frequency data showed the best representation of the normal EKG, with the P, Q, R, S, and T components of the wave all clearly visible.

The 1 Hz cutoff frequency did not give a good visual representation of an EKG, simply because the cutoff frequency was too low. For an EKG to have a frequency of 1 Hz, the heart rate of the patient had to be exactly 60 beats per minute (BPM). And, in order for the filter to behave properly, the patient's heart rate must be below 60 BPM. However, the patient's heart rate at the time of data acquisition was 72 BPM, or 1.2Hz. So, it was possible that the filter could have filtered out parts of the EKG signal as well as the noise. This effect is known as over filtering and causes the filtered signal to not resemble the normal EKG at all.

Looking at the 40 Hz and 70 Hz cutoff frequency graphs, the filtered signal seems to still be heavily corrupted with noise. The cutoff frequencies of these two filters are simply too high. This is especially true for the 70 Hz cutoff frequency, because most ordinary noise components in the room are 60 Hz noise from the flickering of the fluorescent lights. A 70 Hz cutoff frequency would allow that noise component in the pass band.

For all the trials, the specific components of the EKG wave did not deviate in their timing. The P-Q interval on average lasted $0.12\text{-}0.2\text{s} \pm 0.0127$. The RST interval lasted on average $0.35\text{s} \pm 0.0606$. These numbers imply that the waveforms represented on the graphs really are EKGs. Within the 95% confidence intervals, the PQ and the RST intervals are within "normal" EKG timings.

Visually, the 10 Hz cutoff frequency is the best setting for the 2-pole Butterworth filter as illustrated in Figure 1. With a 10 Hz cutoff frequency, the components of the EKG are visible and the noise appears to be removed. However, quantitative data is needed to access any distortion of the signal.

A logistical problem existed in getting a power spectrum analysis for the signals. A power spectrum analysis of the filtered and unfiltered signals would have been the best way to quantify that the EKG results. A power spectrum displays the relative power of each frequency in the frequency domain. The signal peak at 60 Hz (from the fluorescent lighting) would need to be removed from the filtered power spectrum. Additionally, the other aspects of the EKG, notably the 1.2 Hz spike, would need to remain unadulterated.

However, it was not logistically possible, during the project, to re-input the data back into LabView, in order to obtain a power spectrum.

Also without a power spectrum analysis, the individual frequencies of each component of the EKG wave, i.e. the P, QRS complex, and T components, were unknown. Instead, it was assumed that they were all of the same frequency and matched the overall frequency of the EKG wave progression (i.e. 1 Hz or 1.2 Hz). That assumption may or may not be true, because it is possible that the individual wave components to have frequencies other than the normal heart rate.

Phase Angle

Even though it was not possible to get a power spectrum, we were able to use an FFT to analyze the phase of the angle. Looking at Figure 16 from the Results section, the phase shifts are seen to be nearly linear. The phase shifts were regression plotted and found to have a multiple R-value of 0.9998, or nearly 1. Ideal filters linear relationships between cutoff frequency and phase shift. So, from this criterion, our filter behaved ideally.

Improvements to the Lab

The simplest and cheapest way to improve the effectiveness of the filter, is the increase the order of the filter. For this project, a 2 pole, single stage filter was built. This was the one of the simplest filter designs possible, and thus did not yield the best attenuation rate. However to increase the rate of attenuation in the filter, and the increase the sharpness of the “elbow” of the curve, all you have to do is increase the order of the filter from 2 pole to 4 pole or higher. Increasing the number of poles is can be accomplishing by attaching the output of one 2-pole filter to the input of another 2-pole filter, etc. Incorporating additional stages (similar to Ra and Rb in Figure 1) will also increase the sharpness of the elbow as well as the sensitivity of the filter as it increases passband gain. Due to the constraints of the Butterworth filter design, both resistor values (R3) must be adjusted to change the cut-off

frequency. A switch between four filters, with known resistor values and cut off frequencies is suggested.

The other major improvement to the lab would be to have a LabView VI that would generate a power spectrum from already collected data. A new VI should be written to incorporate both filtered and unfiltered power spectrums in addition to the time domain data. This VI should provide four columns of data: filtered and unfiltered voltages (time domain) as well as filtered and unfiltered power spectrums (frequency domain). This would allow the students to quantify their results, thus increasing the validity of the entire experiment.

REFERENCES

1. Bioengineering Laboratory II Manual. *Experiment 2: DC Electronics I and Experiment 3: DC Electronics II*. University of Pennsylvania. Philadelphia, PA. Fall, 1997.
2. Bioengineering Laboratory III Manual. *Experiment 1: EKG and Analog Filtration and Experiment 2: EKG Digital Filtration Analysis*. University of Pennsylvania. Philadelphia, PA. Fall, 1997.
3. DeFatta, David; Lucas, Joseph G.; Hodgkiss, William S. Digital Signal Processing: A System Design Approach. John Wiley & Sons, Inc. New York, NY. 1988.
4. Herpy, M. and Berka, J.-C. Studies in Electrical and Electronic Engineering, Vol. 18: Active RC Filter Design. Elsevier Science Publishing Co., Inc. New York, NY. 1986.
5. Horowitz, Paul and Hill, Winfield. The Art of Electronics, Second Edition. Cambridge University Press. Cambridge, MA. 1989.
6. Johnson, Curtis D. Handbook of Electrical and Electronic Technology. Prentice Hall. Columbus, OH. 1996.
7. Mims, Forrest M. Engineer's Mini-Notebook: Op Amp, IC Circuits, Second Edition, Third Printing. A Siliconconcepts™ Book. 1994.
8. Moore, David S. & McCabe, George P. Introduction to the Practice of Statistics. W. H. Freeman and Company. New York, NY. 1993.
9. One Technology Way. *AD620: Low Cost, Low Power Instrumentation Amplifier*. Norwood, MA. 1997.
10. Strum, Robert D. and Kirk Donald E. Contemporary Linear Systems. PWS Publishing Company. Boston, MA. 1996.
11. Thomas, Roland E. and Rosa, Albert J. The Analysis and Design of Linear Circuits. Prentice Hall. Englewood Cliffs, NJ. 1994.
12. Webster, John G. (ed.). Medical Instrumentation: Application and Design, Second Edition. Houghton Mifflin Company. Boston, MA. 1992.